Experimental Study on High Performance Concrete of Ultra-Deep Mines on the Coast of Eastern China

Daolu Quan (b20180013@xs.ustb.edu.cn)
University of Science and Technology Beijing https://orcid.org/0000-0001-8969-1319
Hongguang Ji
University of Science and Technology Beijing
Xiaobo Su
University of Science and Technology Beijing
Juanhong Liu
University of Science and Technology Beijing
Dongsheng Chen
University of Science and Technology Beijing
Zhen Fu
University of Science and Technology Beijing

Research

Keywords: deep shaft, high performance concrete, stress of supporting structure, concrete strain, on-site monitoring

Posted Date: May 27th, 2021

DOI: https://doi.org/10.21203/rs.3.rs-548510/v1

Experimental study on High performance concrete of ultra-deep mines on the coast of eastern China

QUAN Dao-Lu[1,2], JI Hong-Guang[1,2*], SU Xiao-Bo[1,2], Liu Juan-Hong[1],CHEN Dong-Sheng[1,2],FU Zhen[1,2]

(1 School of Civil and Resource Engineering, University of Science and Technology Beijing, Beijing 100083, China;2 Key Laboratory of Urban Underground Space Engineering, University of Science and Technology Beijing, Beijing 100083, China)

Abstract: To solve the problem of ultra-deep mines on the coast of eastern China under the complex external environment of "high in-situ stress, high osmotic pressure, and strong corrosion", the high-performance concrete shaft wall structure with “high strength and low impact liability” was proposed. The field test study of the high-performance concrete shaft lining was carried out in-1120m ingate and-1114m to-1124m shaft in Sha-ling Gold Mine, and its stress and deformation were monitored and analyzed. Finally, according to the Von-Mises strength criterion and the thick-walled cylinder theory, the calculation formula of bearing capacity of HPC shaft wall was deduced. The results showed that: (1) On the 5th day after in-situ casting, the stress of high-performance concrete tends to be stable. Compared with ordinary concrete, high-performance concrete showed good early strength (2) The high-performance concrete shaft lining strain changes smoothly, and concrete strain can be divided into three stages: rapid growth stage, slow growth stage, and stable stage. (3) Under the external environment of "high in-situ stress, high osmotic pressure, and strong corrosion", the -1120m ingate and -1114m~-1124m shaft lining of Sha-ling Gold Mine supported by high-performance concrete had uniform stress and good mechanical properties, which can provide a reference for similar engineering support design.

Key words: deep shaft; high performance concrete; stress of supporting structure; concrete strain; on-site monitoring

Jiao-dong, located in the eastern peninsula of Shandong Province, is one of the world's three largest gold deposit areas and the largest gold deposit area in China. The proven reserves of gold resources in Jiao-dong are 5000 metric tons [1]. With the intensification of deep resource exploration in the Shandong Peninsula, large deep high-quality deposits in the Jiao-dong coastal area had been discovered successively. To realize the exploitation and utilization of deep resources, China had built a number of deep vertical shafts in coastal areas of Shandong Province during the 13th Five-Year Plan period. For example, the depth of the new main shaft in Xin-cheng Gold Mine is 1527m, the depth of the main shaft in Sha-ling Gold Mine is 1569m, and the depth of the air intake shaft in Sha-ling Gold Mine is 1449m. The auxiliary shaft in Xi-ling mining area of San-san-dao Gold Mine is planned to be 2005m.

Under the complex external environment of "high in-situ stress, high ground temperature, high water pressure, and strong excavation disturbance" [2], the physical and mechanical properties of deep rock mass are generally different from those of shallow rock mass [3-4], and the rock mass changes from elastic state to the plastic state. In the process of shaft excavation, water inrush, rock-burst, lamping, and other engineering support problems are frequent occurrences. In the deep external environment of high in-situ stress and high osmotic pressure, some high-grade shaft lining concrete may even suffer brittle failure. At the same time, the deep strata and deep water quality in the coastal area are rich in Cl^- and SO_4^{2-} ions, and the shaft lining concrete is at risk of chemical corrosion hazards [5-9], which seriously affects the strength and durability of concrete [10-12] and greatly shortening the life of shaft wall. In order to solve the problem of shaft support, many scholars had done a lot of researches. According to the requirements of shaft support under different formation conditions, different forms of shaft support had been proposed, and the stress, deformation, and strength characteristics of shaft wall structure had been studied through model tests [13-19].However, previous studies on the shaft wall support form usually focus on the topsoil section, and there were few reports on the shaft wall stress and deformation

characteristics under the complex external occurrence environment of "high in-situ stress, high osmotic pressure, and strong corrosion" in deep strata.

Based on the -1114m to -1124m section of the air intake shaft and the -1120m ingate high-performance concrete shaft lining structure field application research as the background, the characteristics of high-performance concrete at the scene of the shaft wall stress, deformation analysis. According to the Von-Mises strength criterion and the thick-walled cylinder theory, the calculation formula of bearing capacity of HPC shaft wall was deduced. Summarized the application of high-performance concrete shaft lining structure advantage, and can provide a reference for deep metal shaft wall structure design.

1 Engineering geological

1.1 Engineering background

Sha-ling Gold Mine is located in Zhu-qiao Town, Lai-zhou City, Yantai City, Shandong Province, 10 kilometers west of Lai-zhou Port and 35 kilometers north of Longkou Port. The linear distance between the northwest end of the mining area and the coast of the Bohai Sea is about 5.3 km, which belongs to the coastal area of Shandong Province.

The design depth of the air intake shaft in Sha-ling Gold Mine is 1449m, and the net diameter of the shaft lining is 6.5m, which is excavated by a common method. The design parameters of the shaft wall at -1114m to -1124m of the air intake shaft and the original support of the ingate at -1120m is exhibited in Table 1.

The regional geological structure of the Sha-ling gold mine construction project is complex, and the fault structure is developed in the area, the main fault is the Jiao-jia fault, the branch fault is the Wang-er-shan fault, and the north section fault of Ling-shan . The rock fissures are developed on both sides of the Jiao-jia fault zone. The rock on the hanging wall is dominated by metabgabbro and the footwall is dominated by granite. The maximum horizontal principal stress in the shaft construction engineering area is 24.14MPa ~ 45.56MPa (-775.4m ~ -1532.5m), the minimum horizontal principal stress is 18.85MPa ~ 37.51MPa (-775.4m ~ -1532.5mm), and the maximum horizontal principal stress direction is near NW68.5°.The ion concentration content of groundwater in the survey hole of the air intake shaft is detected, and the ion concentration content is shown in Table 2. According to "Suggestions on the Evaluation Standard of Groundwater Erosion in Metallurgical Industrial Engineering Geological Survey" [20], it can be known that the concrete erosion caused by groundwater in the air intake shaft of Sha-ling Gold Mine belongs to sulfate type erosion. If the original support design scheme is adopted for the shaft lining from -1114m to -1124m of the air intake shaft and the ingate from -1120m, the concrete will face the harm of sulfate erosion, and the groundwater contains Cl^-, which will also cause the steel bar embroidery erosion.

Table 1 Original support parameters of-1114m to-1124m shaft wall and-1120m ingate of downcast shaft

Deep	Support parameter	
	primary support	Second times support
-1120m ingate	Bolt type:MSGLW-335/20×2000;Bolt density :1m×1m; Butterfly tray:150×150×10;Density of steel mesh:120×120，Rebar diameter:6mm;	C30 reinforced concrete, support thickness:400mm; Outer reinforced:HΦ22@250VΦ18@250; Inner reinforced:HΦ22@250VΦ18@250; Stirrup:Φ10@500*500;
-1114m to -1124m	No	Ditto

Table 2 The results of ion concentration detection in downcast shaft of Shaling Gold Mine

Ion	Cl^-	NO_3^-	SO_4^{2-}	HCO_3^-	K^+	Na^+	Ca^{2+}	Mg^{2+}	Fe^{3+}
	/ mg·L^{-1}	/ mg·L^{-1}	/ mg·L^{-1}	/ mg·L^{-1}	/ mg·L^{-1}	/ mg·L^{-1}	/ mg·L^{-1}	/ mg·L^{-1}	/ mg·L^{-1}

content	1779.20	5	584.04	215.17	288.32	972.55	160.32	97.24	0.36

2 Field test

The high-performance concrete of the deep shaft is composed of silicate 42.5R cement, special compound, river sand, copper-plated microwire steel fiber, polycarboxylic acid water reducer. The mix ratio of high-performance concrete in the deep shaft is present in Table 3. The compound is composed of finely ground slag powder, fly ash, and silica fume proportions and its performance meets the requirements of concrete cementing materials. Liu Juan-hong et al. [21] had studied the splitting tensile strength, flexural strength, brittleness coefficient, impact energy index, dynamic failure time, and other parameters of HPC through laboratory tests. The brittleness coefficient, impact energy index, dynamic failure time, and other parameters of HPC belong to the category of non-impact liability, which will not be elaborated in detail in this paper.

In order to complete the field test research on the -1120m ingate of the air intake shaft (the ingate support is 5m) and the -1114m to -1124m high performance concrete (HPC) shaft lining, about 120m^3 high performance concrete (HPC) was prepared on site. The high performance concrete was mixed evenly with a mixer on the surface and transported to the casting layer through a bucket. When concrete was mixed, steel fiber was added in batches to make it evenly dispersed to ensure the workability of concrete. The HPC after mixing is shown in Fig. 1, and the HPC shaft lining after mold removal is shown in Fig. 2.

Table 3 Mix proportion of high performance concrete

Cement / kg·m^{-3}	Special admixtures / kg·m^{-3}	Sand / kg·m^{-3}	Steel fibre / kg·m^{-3}	Water / kg·m^{-3}	Admixture / kg·m^{-3}	water-binder ratio
240	630	1205	50	200	10	0.23

Fig.1 High performance concrete after mixing

Fig.2 High performance concrete shaft wall after form stripping

2.1 Field monitoring instrument

2.1.1 Force measuring bolt

The environment of the deep shaft in coastal areas is harsh, and the complex external environment, such as high ground temperature, water drench from large shaft wall, and enhanced chemical corrosion, puts forward higher requirements for the reliability and durability of monitoring instruments. To cope with the complex external environment of the deep shaft and ensure the authenticity and reliability of the monitoring results, the improved stress monitoring sensor, force measuring bolt, was used to monitor shaft wall stress. As shown in Fig. 3, the force measuring bolt is composed of four parts: steel bar meter, steel bar, and a steel plate in PVC pipe. The steel bar meter is connected to both ends of the steel bar, one end of the steel bar is welded steel plate. The steel plate length × width: 150×150 mm, the thickness is 6mm. The force measurement bolt is 900 mm long.

Before the concrete shaft wall is poured, one end of the unconnected steel plate is fixed on the surrounding

rock, and the steel bar deep into the surrounding rock is fixed in the surrounding rock by epoxy resin. Both ends of the PVC pipe are sealed to avoid the reinforcement meter being interfered with by the shaft wall concrete pouring vibration and reduce the probability of the reinforcement meter being corroded by groundwater. This instrument had been used in stress monitoring of new main shaft at -1300m and -1418m levels in Xin-cheng Gold Mine, and its reliability had been proved [22].

The concrete strain monitoring sensor adopts the embedded vibrating string concrete strain gauge. The standard measuring range of the embedded vibrating string concrete strain gauge is ±3000, and the working environment temperature is -25~80℃, with the temperature measuring function.

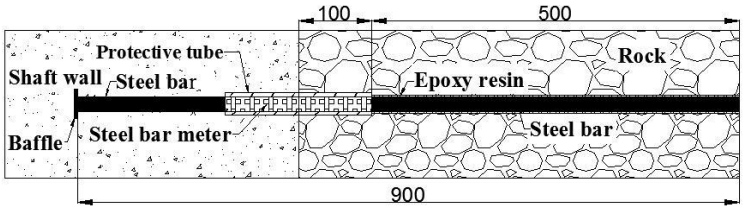

（a）Monitoring diagram of force-measuring anchor

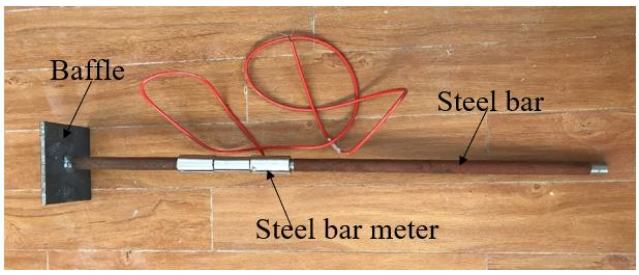

（b）Image of force-measuring anchor

Fig.3 Force-measuring anchor

2.2 Test point arrangement

As illustrates in Fig. 4. The layout of stress and strain monitoring points on the shaft lining from -1114m to -1124m of the air intake shaft and the ingate from -1120m. Three measuring points were arranged at the arch and the left and right shoulder of ingate at 1120m; Three measuring points were arranged on the shaft wall connected with the horse head door, and the three measuring points on the shaft wall were at the same level with the waistline of the horse head door (-1117.7m). One load bolt, one circumferential concrete strain gauge, and one axial concrete strain gauge were installed at each measuring point. Data collection will be carried out after concrete pouring, and 3 ~ 4 groups of data will be collected at each measuring point for a total of 30 days.

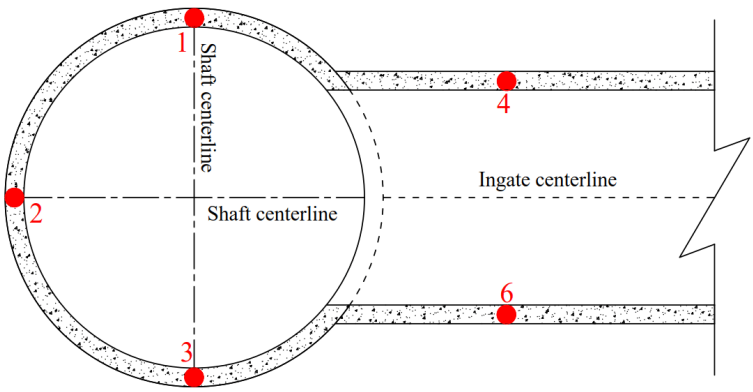

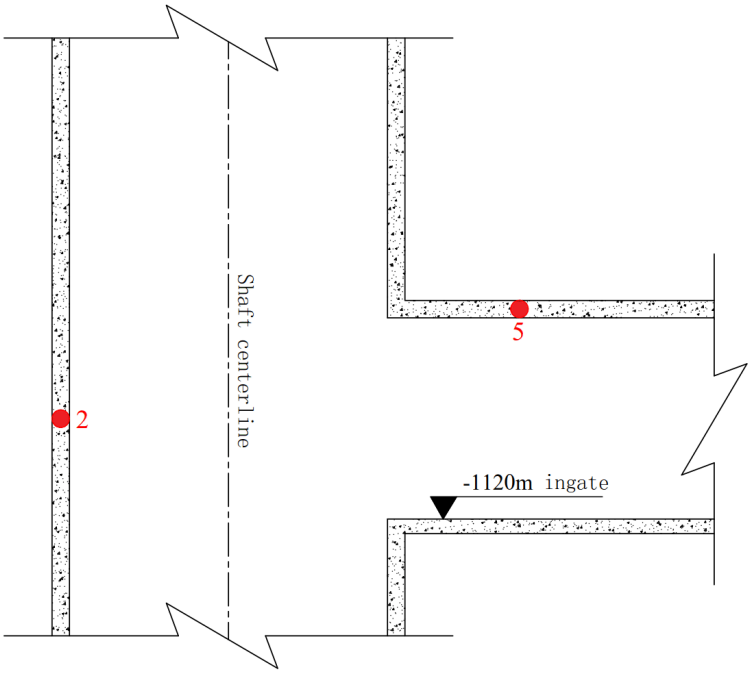

Fig.4 Layout of measuring points

3 Test results and analysis

3.1 Shaft wall stress characteristics and analysis

The shaft wall stress variation of HPC at-1117.7m level in Sha-ling Gold Mine was shown in figure 5. As can be seen from Fig. 5, the stress of the three measuring points on the shaft wall fluctuated from September 20 solstice to September 24. No. 1 was subjected to tensile stress, while No. 2 and No. 3 were subjected to compressive stress. With the hydration of cementing materials, the concrete gradually changes from the flow state to the plasticity state after the casting of HPC. At the same time, the strength of HPC is increasing, and the non-uniform deformation of concrete were generated due to the uneven volume expansion, which maked the supporting reaction force of the surrounding rock on the shaft wall in a dynamic change.

On the fifth day after the casting of HPC, the stress at measuring points No. 1, No. 2, and No. 3 of the shaft wall begin to stabilize, and the strength of HPC doesn't change. When ordinary concrete was used for shaft wall support, the strength of concrete at the 7-day age reaches 70% to 80% of the standard strength, and the shaft wall stress began to stabilize. However, the strength of HPC doesn't change on the 5th day after casting, and HPC shows early strength characteristics. The stress of the three measuring points on the -1117.7m HPC shaft wall is consistent in time and space, which shows the excellent performance of HPC in the complex external environment of "high in-situ stress, high osmotic pressure, and strong corrosion" in deep metal mine.

After October 8, the shaft wall compressive stress at the No.3 measuring point increased from 0.6MPa to 1.8MPa. Analysis shows that the cause of this phenomenon were related to the increase of water pressure. The horizontal pressure of the shaft wall combined with the surrounding rock is composed of water pressure and rock pressure [23]. Based on the surrounding rock conditions revealed on the project site, the surrounding rock of -1116~-1120m of the air intake shaft was broken and fractures are developed, and the water inflow of the rock was about 4.7$m^3 \cdot h^{-1}$. With the shaft excavated, the rock swelling effect after excavation and unloading opens the fracture [24]. The opening of the crack increases the underground water pressure, and the deformation of the surrounding rock increases the horizontal pressure on the shaft wall.

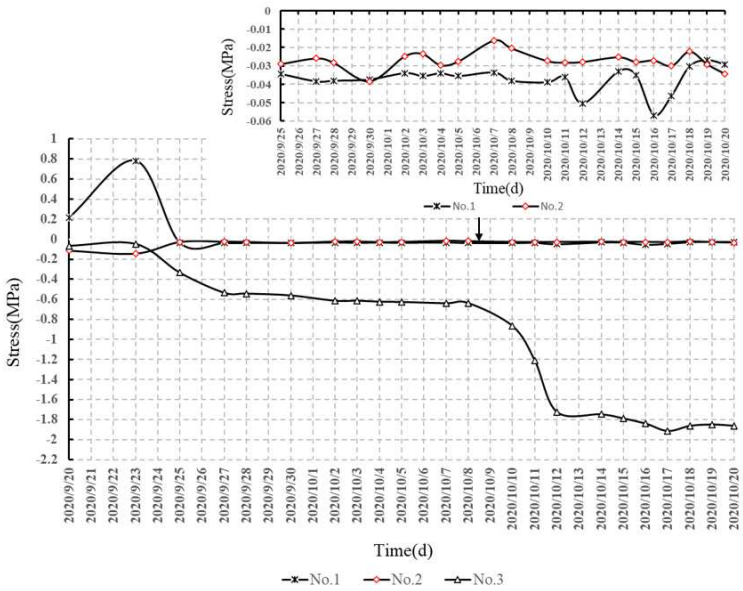

Fig.5 Concrete stress change of -1117.7m shaft lining

The stress changes at the three measuring points of the -1120m ingate of the arch and the left and right shoulder of Sha-ling Gold Mine are shown in Fig. 6. As can be seen from Fig. 6, within 30 days after the concrete pouring of the ingate, the three measuring points of the ingate were subjected to tensile stress, which was always fluctuating. At ingate, the maximum tensile stress at No.4 measuring point is 2.2MPa, No. 5 measuring point is 2.3MPa, and No. 6 measuring point is 2.4MPa. When the HPC is gradually consolidated and released heat by hydration, the stress at the three measuring points of the arch and the left and right shoulder of ingate is in a fluctuating state. At the same time, as a special "geographical location" of the connecting section between the roadway and the shaft, with the continuous excavation of the shaft, the stress of the surrounding rock of the ingate is constantly adjusted, the stress of surrounding rock on the shaft wall is constantly changing, and the stress of the ingate is in a fluctuating state.

The maximum horizontal principal stress of -1121m in Sha-ling gold deposit is 34.09MPa, and the vertical principal stress is 29.65MPa, which is 1.15 times that of the vertical principal stress. The maximum principal stress direction is near the NW direction. Influenced by the distribution of in-situ stress field in the Sha-ling Gold Mine construction area, the three measuring points of ingate vault and left and right arches are all subjected to tensile stress. The opening of the ingate of the air inlet shaft in Sha-ling Gold Mine is due south, and the Angle with the direction of the maximum principal stress is about 45°. The vertical principal stress at the arch and left and right shoulder of ingate is less than the maximum horizontal principal stress. Therefore, the surrounding rock of ingate under the maximum horizontal principal stress will be greater than the vertical principal stress. With the excavation of the lower shaft, the surrounding rock stress is constantly released, and the maximum horizontal principal stress of ingate surrounding rock is more obvious than that of the vertical principal stress. Under the compression of the maximum horizontal principal stress, the surrounding rock and shaft wall at the arch and abutment of ingate exhibit "opposite" movement, which causes tensile stress at the arch and abutment of ingate.

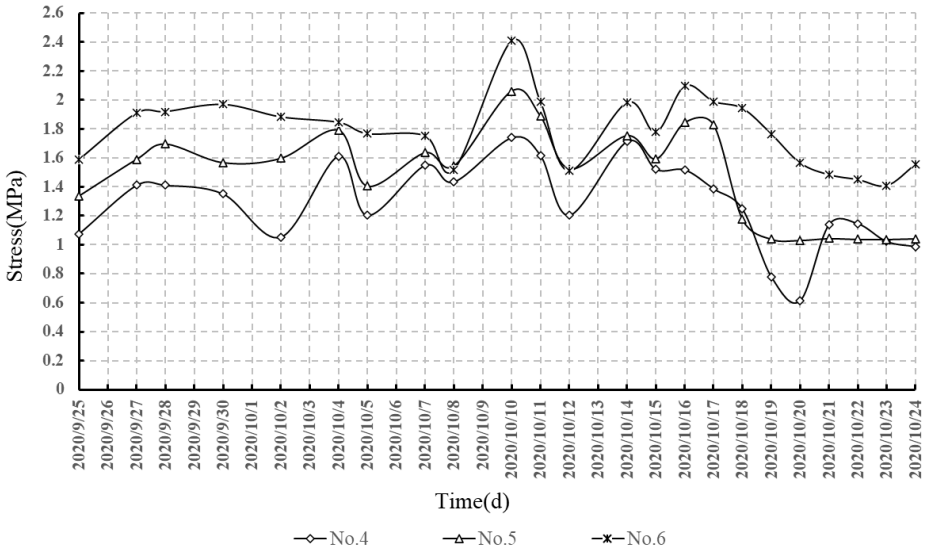

Fig.6 Concrete stress change of -1120m ingate

3.2 Variation and analysis of concrete strain

As shown in Fig.7 (a)~(b), the strain variation of HPC in shaft wall of -1117.7m in Sha-ling Gold Mine. The axial concrete strain gage at measuring point No. 2 and the circumferential concrete strain gage at measuring point No. 3 are damaged and no data has been collected. On the whole, the concrete strain at the three measuring points of the HPC shaft wall shows a trend of first increasing and then stabilizing. The strain change can be divided into three stages: rapid growth stage, slow growth stage, and stable stage.

The strain growth rate from day 7 to day 8 to 28 after the completion of the casting of the HPC shaft wall is defined as

$$\varepsilon_{7D}=\frac{\varepsilon_7-\varepsilon_1}{\varepsilon_1}\times 100\% \quad (1)$$

$$\varepsilon_{28D}=\frac{\varepsilon_{28}-\varepsilon_8}{\varepsilon_8}\times 100\% \quad (2)$$

Where: ε_{7D} is the strain growth rate of the HPC shaft wall from the completion of pouring to the 7th day; ε_{28D} is the strain growth rate from the 8th day to the 28th day after the casting of the HPC shaft wall; ε_1 is the strain value of high-performance concrete after pouring, $\mu\varepsilon$; ε_7 is the 7th-day strain value of HPC, $\mu\varepsilon$; ε_8 is the 8th-day strain value of HPC, $\mu\varepsilon$; ε_{28} is the 28th-day strain value of HPC, $\mu\varepsilon$。

According to Fig. 7 (a) and (b), the strain growth rate from the 7th day to the 8th day to the 28th day after the completion of the casting of the HPC shaft wall can be calculated, as shown in Table 4.

Table 4 Strain growth rate of HPC shaft lining

Measuring point	ε_{7D}	ε_{28D}
The circular strain of measuring point No. 1	105%	18%
The circular strain of measuring point No.2	92%	25%

The axial strain of measuring point No. 1	42%	8%
The axial strain of measuring point No. 3	-10%	3%

As can be seen from the table 4, from the completion of casting of HPC shaft wall to the 7th day after casting, the growth rate of circumferential strain at measuring point No. 1 and No. 2 both exceeded 90% and the increase rate of axial strain at measuring point No. 1 was 42%. Except for the negative axial strain growth rate at the No. 3 measuring point, the strain growth rate of concrete at other measuring points ranged from 42%-105%. The strain of high-performance concrete is in the stage of rapid growth. After the casting of high-performance concrete, under the constraint of surrounding rock, the cementing material is hydrated and the self-generated volume deformation of concrete is generated. As the strength of concrete increases, the constraint of surrounding rock increases, and the strain of concrete increases rapidly.

The concrete strain increases slowly from the 8th day to the 28th day after the high performance concrete is poured. The growth rate of the circumferential strain at measuring point No. 1 and No. 2 is 18-25%. The growth rate of the axial strain at measuring point No. 1 and No. 3 is less than 10%, and the strain growth rate of HPC is significantly reduced. After pouring high-performance concrete for 7 days, the strength of concrete continues to increase with the progress of hydration. Under the condition that the acting stress of surrounding rock on concrete shaft wall remains unchanged, with the decrease of stress strength ratio, the movement of cementitious particles in concrete decreases. As the cementitious body transfers from a disordered state to an ordered state, the deformation of concrete decreases, and the increasing trend of the strain of concrete slows down.

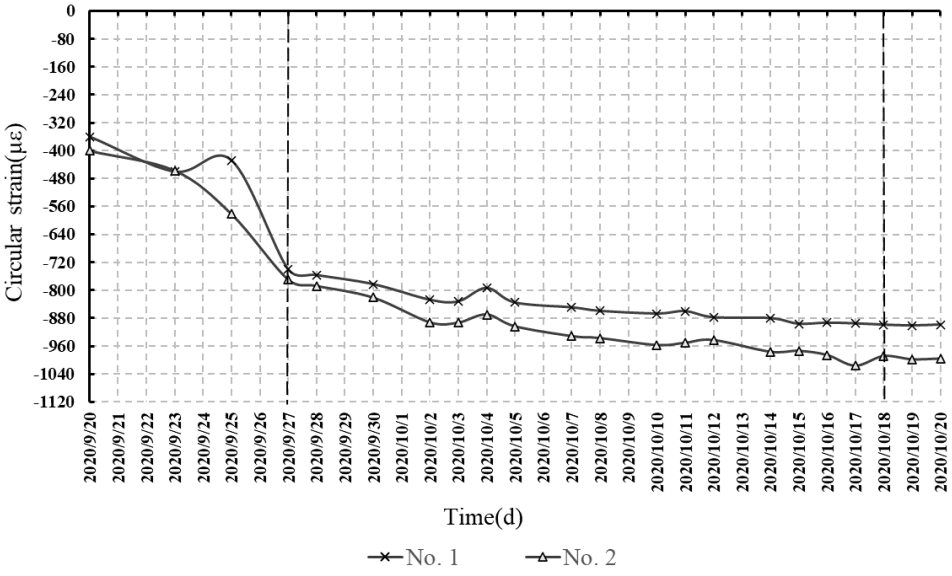

(a) Circumferential strain of high performance concrete

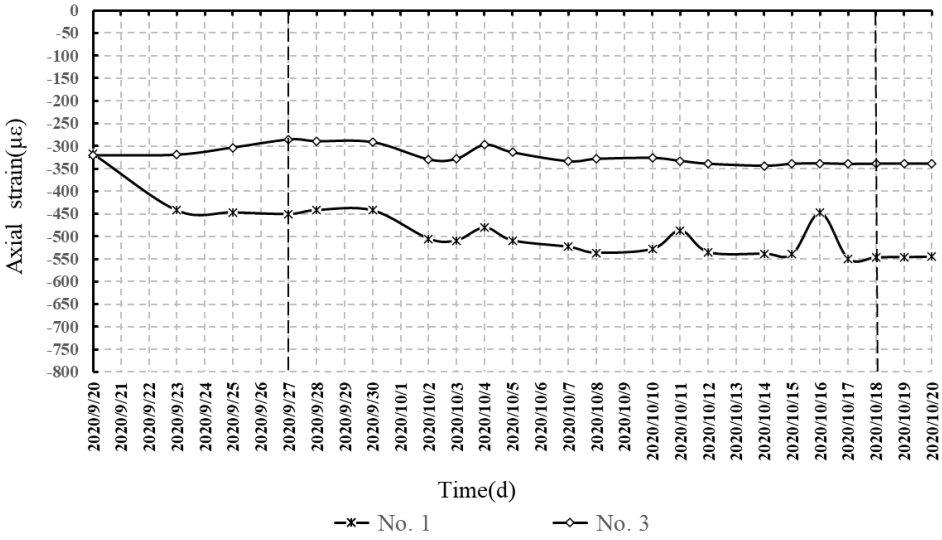

(b) Axial strain of high performance concrete

Fig. 7 Strain variation of high performance concrete at -1117.7m level

Fig. 8 (a) and (b) show the changes of the annular and axial strain of HPC at -1120m ingate of Sha-ling Gold Mine. As can be seen from Fig. 8, the circumferential strain of HPC at measuring points 4 and 5 of ingate is compressive, while the circumferential strain of concrete at measuring points 6 is tensile. The axial strain of HPC at measuring points 4, 5, and 6 are all the compressive strain. The strain variation law of -1120m high-performance concrete of ingate is consistent with that of -1117.7m high-performance concrete of shaft wall: The concrete strain increases rapidly from the completion of casting to the 7th day after casting. The concrete strain increases slowly from the 8th day to the 28th day after casting. After 28 days, the concrete strain is in a stable stage, and the strain does not change. Compared with the strain change of shaft wall concrete at -1117.7m, the strain growth rate of -1120m high-performance concrete at ingate in the first 7 days is lower and the strain change of concrete is more stable.

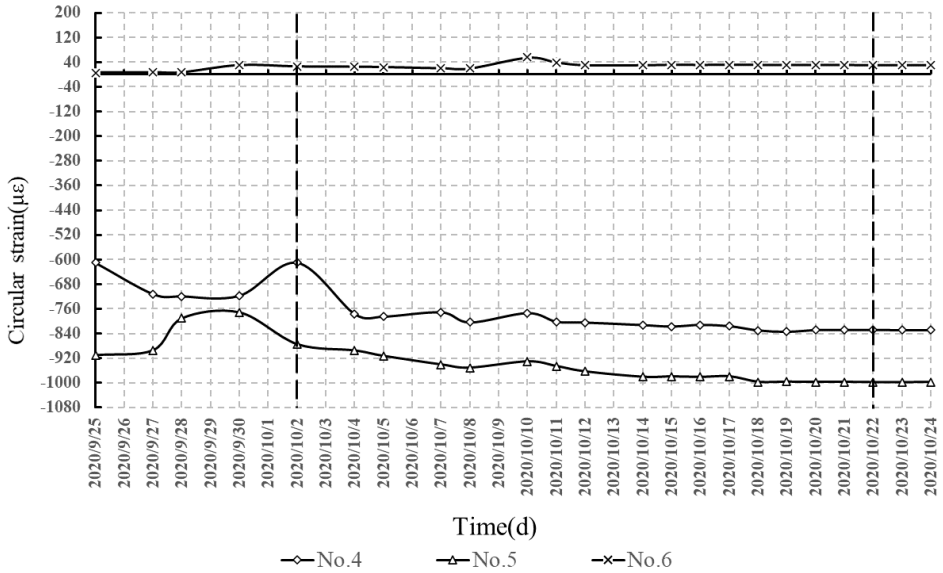

(a) Circumferential strain of high performance concrete for ingate

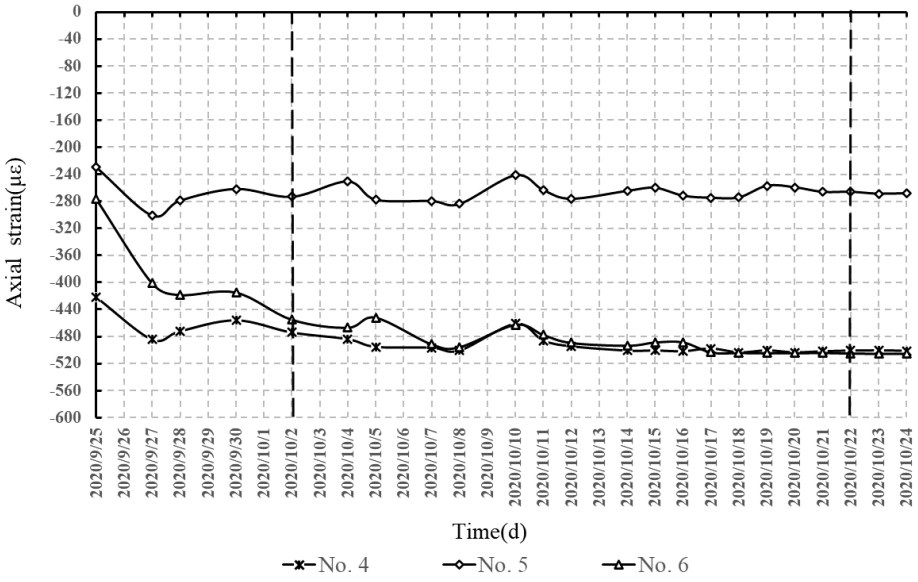

(b) Axial strain of high performance concrete for ingate

Fig.8 Strain variation of high performance concrete for -1120m ingate

4 Analysis of mechanical advantage of field application of high-performance concrete sidewall

4.1 Mechanism analysis of early strength of high-performance concrete shaft wall

As can be seen from Fig. 4, on the fifth day after the HPC casting, the forces at the three measuring points of the shaft wall tended to be stable. However, the new main shaft wall of Xin-cheng Gold Mine (-1300m), which is also located in the Jiao-jia fault zone, is supported by C40 plain concrete, and the force on the shaft wall is always fluctuating within 26 days after concrete pouring [22]. Compared with the common concrete, the time of stability of the HPC shaft wall is shortened, and HPC shows good early strength.

The early strength of HPC shaft wall is related to two factors :(1) HPC adopts polycarboxylic acid superplastifier. The addition of high performance water reducer reduces the amount of water and reduces the water-binder ratio of high performance concrete. High performance concrete shows good early strength. (2) there is a large amount of silica fume in the special mixture of high-performance concrete, and the gap between the high purity SiO_2, cement particles in the silica fume is filled with silica fume, which speeds up the hydration reaction of cement, produces a large number of cementitious products in the early stage of hydration, and improves the compactness of the paste, thus improving the early strength of concrete.

4.2 Mechanism analysis of low impact liability of high-performance concrete shaft wall

The low impact liability of HPC is reflected in the uniform stress of HPC shaft wall structure and the stable strain change of HPC.As can be seen from Fig. 4, the stress properties of the three measuring points at -1111.7m monitoring section are the same, and the stress values are almost the same. The force of the -1120m high performance concrete shaft wall of the ingate also has similar characteristics. Under the influence of high in-situ stress and strong excavation disturbance, the force of HPC shaft wall is uniform, which reduces the stress concentration effect and cuts off the path of sudden energy release of a certain point in concrete under the action of concentrated force. The strain change of high-performance concrete shaft wall is stable, and there is no strain sharp increase or continuous fluctuation, which indicates that the ability to accumulate elastic strain energy in high-performance concrete is poor, then the elastic strain energy that can be released by high-performance concrete can’t reach the energy needed for its failure.

The low impact liability of HPC shaft wall is related to three factors :(1) there is no coarse aggregate in HPC, the concrete has good fluidity, and the scale of internal fabric interface decreases, which increases the compactness of concrete. (2) Steel fiber has a toughening effect on concrete. When steel fiber is added to high-performance concrete, the ultimate stress and ultimate strain of concrete will increase. At the same time, steel fibers are interwoven and bonded in the shaft wall, which can effectively prevent the expansion of cracks and slow down the development of micro-cracks in concrete [25]. The friction effect of the interface between the fiber and concrete and the tension effect of the fiber itself weaken the deformation energy storage of the concrete itself. (3) high-performance concrete special composite contains fly ash, mineral powder. With the addition of fly ash and mineral powder, the autogenous shrinkage of concrete at the early stage is significantly reduced, and the ability of concrete to resist creep is enhanced. The autogenous volume deformation and dry shrinkage deformation of HPC are reduced, and the strain change of concrete is stable.

5 Theoretical analysis of the ultimate bearing capacity of the high-performance concrete shaft wall

For the determination of the bearing capacity of a high-performance concrete shaft wall, there is no reasonable calculation formula at present. Therefore, according to the design code of the mine shaft and chamber in China, the fourth strength theory is recommended to be adopted, and the calculation formula of the ultimate bearing capacity of the HPC shaft wall is derived by combining the thick-walled cylinder theory.

5.1 Theory of concrete strength

Domestic and foreign scholars have put forward various concrete strength theories, which are mainly divided into classical strength theory and modern strength theory [26]. The classical strength theory mainly includes four strength theories, while the modern strength theory is mostly obtained by parameter fitting based on a large number of experimental data. The representative ones are Bresler-Pister, Willam-Warnke, Otteosen, Hsieh-Ting-Chen, Guozhenhai-Wang Chuanzhi strength criterion.The fourth strength theory, namely Von-Mises yield theory, is suggested to be adopted in the design code of mine shaft and chamber in China. The Von-Mises intensity criterion is expressed as

$$\sqrt{\left(\sigma_1\text{-}\sigma_2\right)^2+\left(\sigma_1\text{-}\sigma_3\right)^2+\left(\sigma_2\text{-}\sigma_3\right)^2}\le\sqrt{2}f_c \qquad (1)$$

Where: σ_1 is the first principal stress; σ_2 is the second principal stress; σ_3 is the third principal stress; Taking the tensile stress as positive. f_c is the axial compressive strength of concrete prism.

5.2 Theoretical analysis

It is assumed that the shaft wall is homogeneous and continuous isotropic material. According to the force law of thick-walled cylinder, the stress solution of the shaft wall under the action of external pressure is[27]

$$\sigma_r=-\frac{b^2p}{b^2-a^2}\left(1-\frac{a^2}{r^2}\right) \qquad (2)$$

$$\sigma_\theta=-\frac{b^2p}{b^2-a^2}\left(1+\frac{a^2}{r^2}\right) \qquad (3)$$

$$\sigma_z=\nu\left(\sigma_r+\sigma_\theta\right) \qquad (4)$$

Where： a is the inner radius of the shaft wall; b is the outer radius of the shaft wall,， p is the uniform

external pressure borne by the shaft wall; σ_r is the normal stress of the shaft wall; σ_θ is the tangential stress of the shaft wall; σ_z is the vertical stress of the shaft wall; ν is the Poisson's ratio of the shaft wall; Order $\nu = 0.5$, and $\sigma_r > \sigma_z > \sigma_\theta$.

Formula (2) ~ (4) was substituted into Formula (1) of Von-Mises strength criterion

$$p = \frac{f_c r^2 \left(b^2 - a^2\right)}{\sqrt{3} a^2 b^2} \qquad (5)$$

Since the concrete enters the plastic state in the first place, without considering the stress concentration of concrete, the ultimate pressure of concrete is

$$p = \frac{f_c \left(b^2 - a^2\right)}{\sqrt{3} b^2} \qquad (6)$$

According to Formula 6, the axial compressive strength of HPC is certain, and the ultimate bearing capacity of the shaft wall is related to the inner and outer radius of the shaft wall. Therefore, a reasonable thickness-diameter ratio should be selected according to the ground pressure in the design of HPC support to achieve the best supporting effect.

6 Conclusion

The maximum compressive stress of HPC sidewall structure at the -1117.7m level of the air shaft in Sha-ling Gold Mine is 1.95MPa. The tensile stress of HPC shaft wall structure at the arch of the ingate and the left and right shoulder of the air intake shaft at -1120m is 2.4MPa, which is influenced by the maximum principal stress in Sha-ling Gold Mine. Shaft walls at the arch of ingate and left and right shoulder of the air intake shaft at -1120m are separated from the surrounding rock, and phase back movement occurs, resulting in tensile stress on the shaft wall at the arch and left and right shoulder. Compared with common concrete, the stress time of HPC shaft wall tends to be stable for about 2 days, and HPC shows good early strength characteristics.

According to the measured strain data of HPC at six measuring points of the -1117.7m shaft wall, the -1120m arch, and the left and right arches of the air inlet shaft in Sha-ling Gold Mine, the strain change of the HPC shaft wall is stable, and the strain change can be divided into three stages: rapid growth stage, slow growth stage and stable stage. The circumferential strain growth rate of the HPC shaft wall is greater than the axial strain growth rate.

The high-performance concrete (HPC) shaft wall structure has good early strength and low impact tendency under the environment of "high ground stress, high osmotic pressure, and strong corrosion", and can meet the complex and harsh requirement of supporting the metal mine depth shaft in a coastal area, so it is an ideal supporting structure for the metal mine depth shaft. It has a certain reference value to the design and engineering application of the shaft wall structure of the deep metal mine shaft.

Acknowledgements

This work was supported by National Natural Science Foundation of China.(grant numbers 51534002); The State Key Research Development Program of China (Grant numbers 2016YFC0600801);The authors of this article are so grateful to the anonymous reviewers for their valuable comments and modification suggestions on the improvement of this paper.

Data Availability

The data used to support the findings of this sturdy are available from the corresponding author upon request.

Conflicts of Interest

The author declare that they have no Conflicts of interest.

References

[1] SONG Ming-Chun, LIN Shao-Yi, YANG Li-Qiang, et al. Metallogenic model of Jiaodong Peninsula gold deposits [J]. Mineral Deposits, 2020,39(02):215-236.

[2]He Man-chao, Xie He-ping, Peng Su-ping, et al. Study on rock mechanics in deep mining engineering [J]. Chinese Journal of Rock Mechanics and Engineering, 2005 (16): 2803-2813.

[3]Zhang Liu, Wang Sheng-zu, Shi Liang-qi. Strength characteristics of six kinds of rocks in China under high confining pressure [J]. Chinese Journal of Rock Mechanics and Engineering, 1985 (01): 10-19.

[4]Zhou Hongwei, Xie He-ping, Zuo Jian-ping. Research Progress of Rock Mechanical behavior under deep high ground stress [J]. Advance in Mechanics, 2005 (01): 91-99.

[5] Leemann A，Loser R. Analysis of concrete in a vertical ventilation shaft exposed to sulfate-containing groundwater for 45 years［J］. Cement ＆ Concrete Composites，2011，33(1) : 74－83.

[6] Elke Gruyaert, Philip Van den Heede, Mathias Maes et al, Investigation of the influence of blast-furnace slag on the resistance of concrete against organic acid or sulphate attack by means of accelerated degradation tests,Cement and Concrete Research,Volume 42, Issue 1,2012,Pages 173-185,ISSN 0008-8846,https://doi.org/10.1016/j.cemconres.2011.09.009.

[7] Zhao Li, Liu Juanhong, Zhou Weijin, et al. Evolution and Mechanism Analysis of corrosion damage of concrete Materials in Mine Environment [J]. Journal of Coal, 2016,41 (6): 1422- 1428.

[8] Liu Juanhong, Bian Libo, He Wei, et al. Investigation and failure mechanism of concrete shaft lining corrosion in coal mine [J]. Journal of Coal, 2015,40 (3): 528-533.

[9]Yu-cheng Zhou, Juan-hong Liu, Shun Huang, et al. Performance change of shaft lining concrete under simulated coastal ultra-deep mine environments, Construction and Building Materials, Volume 230,2020,116909,ISSN09500618,https://doi.org/10.1016/j.conbuildmat.2019.116909.

[10]Li Xurong, Ji Hongguang, Wang Jun et al. Test Research on Strength Damage of Concrete Shaft Lining under Salt Disaster Corrosion[J].Metal Mine, 2014(10):157-160.

[11] XU Hui, CHEN Zhan-qing, GUO Xiao-qian. Physical and mechanical performance and influencing factors of high performance concrete under sulfate attack[J]. Journal of Coal, 2012,37(02):216-220.

[12] Zhong-ya Zhang, Xiao-guang Jin, Wei Luo, Long-term behaviors of concrete under low-concentration sulfate attack subjected to natural variation of environmental climate conditions, Cement and Concrete Research, Volume 116,2019,Pages 217-230,ISSN 0008-8846, https://doi.org/10.1016/j.cemconres.2018.11.017.

[13] ZHOU Xiao-min, ZHOU Guo-qing, HU Qi-sheng, et al. Model test research on shaft lining built in high pressure rock aquifer[J].Chinese Journal of Rock Mechanics and Engineering, 2011,30(12):2514-2522.

[14] YAO Zhi-shu, YU Gui-hua, CHENG Hua, et al. Research on vertical bearing capacity of shaft lining structure of high strength concrete and double steel cylinders in super-thick alluvium[J]. Rock and Soil Mechanics, 2010,31(06):1687-1691.

[15] YAO Zhi-shu，CHENG Hua，RONG Chuan-xin. Experimental study on shift-boring lining of high performance concrete and double steel cylinder in super-deep alluvium[J].Chinese Journal of Rock Mechanics and Engineering, 2007(S2):4264-4269.

[16] YAO Zhi-shu, CHENG Hua, JU Xian-bo. Research and application of high strength steel fiber concrete compound shaft lining with inner steel plate in deep alluvium shaft repair[J].Journal of China Coal Society, 2017,42(09):2295-2301.

[17] RONG Chuan-xin, WANG Xiu-xi, CHENG Hua. Research on mechanical characteristics of high-strength

reinforced concrete shaft lining in deep alluvium[J]. Chinese Journal of Rock Mechanics and Engineering, 2008(S1):2841-2847.
[18]YAO Zhi-shu. An experimental study on steel fiber reinforced high strength concrete shaft lining in deep alluvium[J]. Chinese Journal of Rock Mechanics and Engineering, 2005(07):1253-1258.
[19]HAN Ta, YANG Wei-Hao, REN Yan-long. Horizontal ultimate bearing capacity of encased steel concrete shaft lining[J]. Journal of Mining and Safety Engineering,2011,28(02):181-186.
[20] Ministry of Metallurgical Industry Nanchang Nonferrous Metallurgy Design Institute. Metallurgical mine tunnel design reference, Volume 1 (tunnel engineering) [M]. Metallurgical Industry Press, 1979.
[21] ZHOU Yucheng, LIU Juan-hong, JI Hong-guang, et al. Study on Bursting Liability of Fiber Reinforced Shaft Lining Concrete Based on Temperature and Compound Salt[J].Materials Reports, 2019,33(16):2671-2676.
[22]Quan Dao-lu, Ji Hong-guang, Su Xiao-Bo, et al. Monitoring and Result Analysis of Pressure in Deep Vertical Shaft of Metal Mine by Force Measuring Anchor Bolt[J].Metal Mine, 2019(06):57-61.
[23] Link. Principles of shaft wall calculation in unstable rock formation [M]. Coal Industry Press, 1979.
[24] H.M. Petuhov. Rock burst in coal mine [M]. Coal Industry Press, 1980.
[25]Liu Yong-shen, Wang Xiao-jun, Jin Ting, et al. Study on the mechanical properties and constitutive relation of steel fiber reinforced concrete[J].Journal of University of Science and Technology of China,2007(07):717-723.
[26]DING Fa-xing, WU Xia, XIANG Ping, et al. Reviews on strength theories of concrete and isotropic rock[J]. Engineering Mechanics,2020,37(02):1-15.
[27]Lu Mingwan, Luo Xuefu. Theory Basis of Elasticity [M]. Beijing: Tsinghua University Press, 2001:189-191.

Figures

Figure 1

High performance concrete after mixing

Figure 2

High performance concrete shaft wall after form stripping

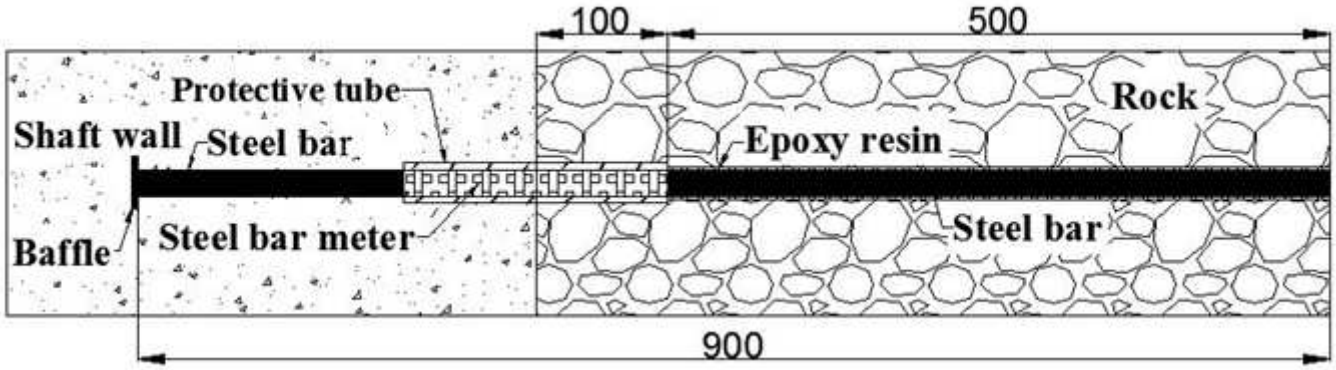

（a）Monitoring diagram of force-measuring anchor

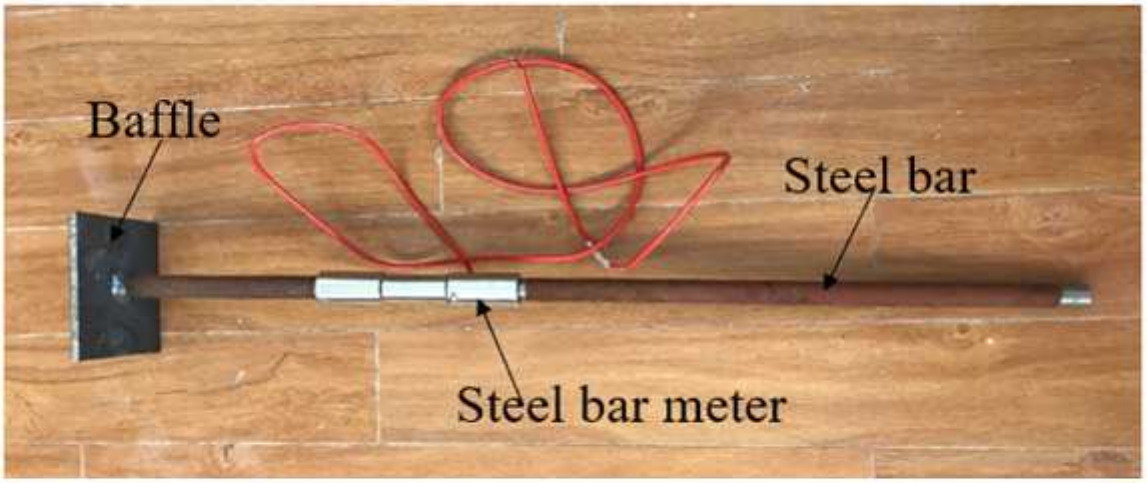

（b）Image of force-measuring anchor

Figure 3

Force-measuring anchor

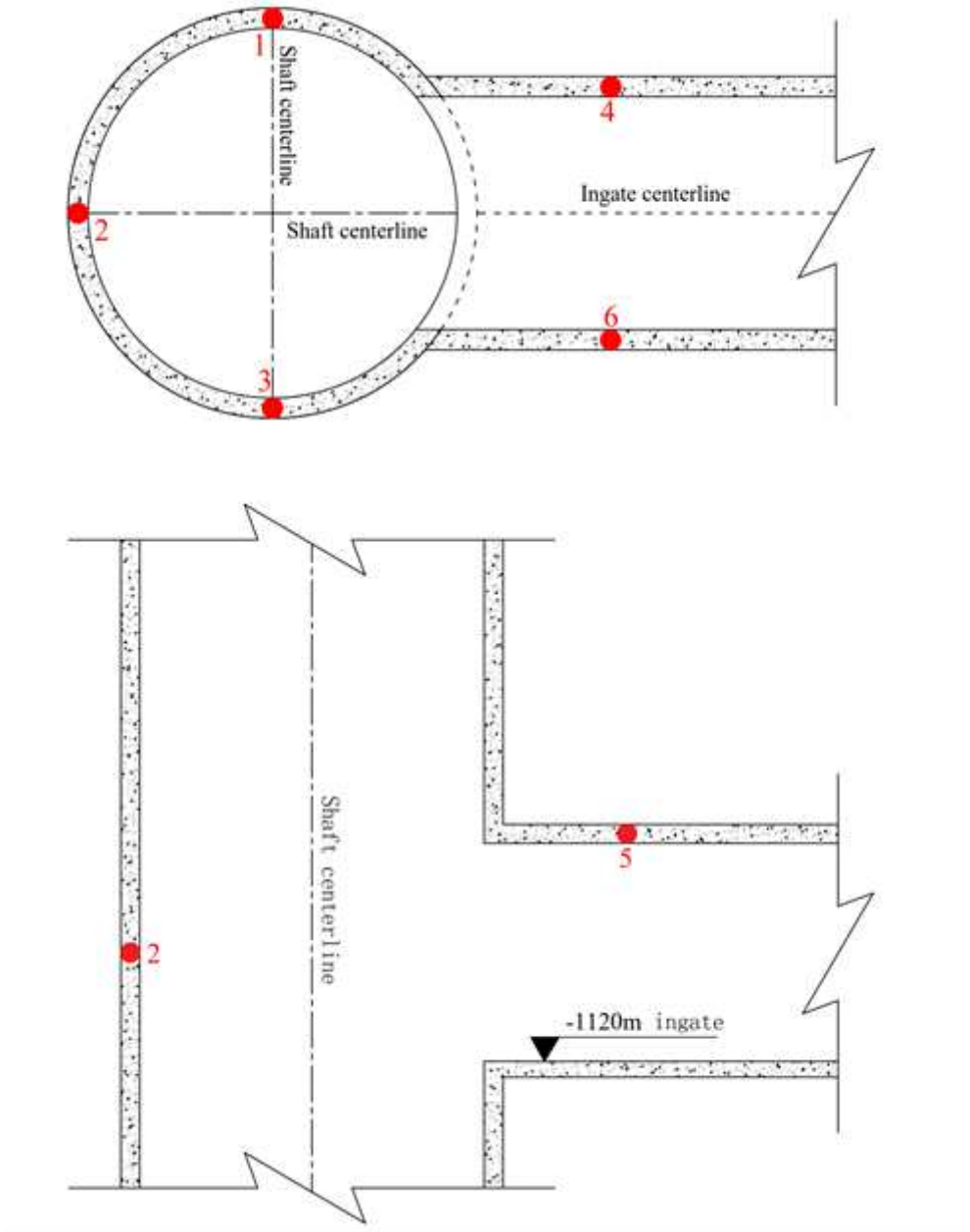

Figure 4

Layout of measuring points

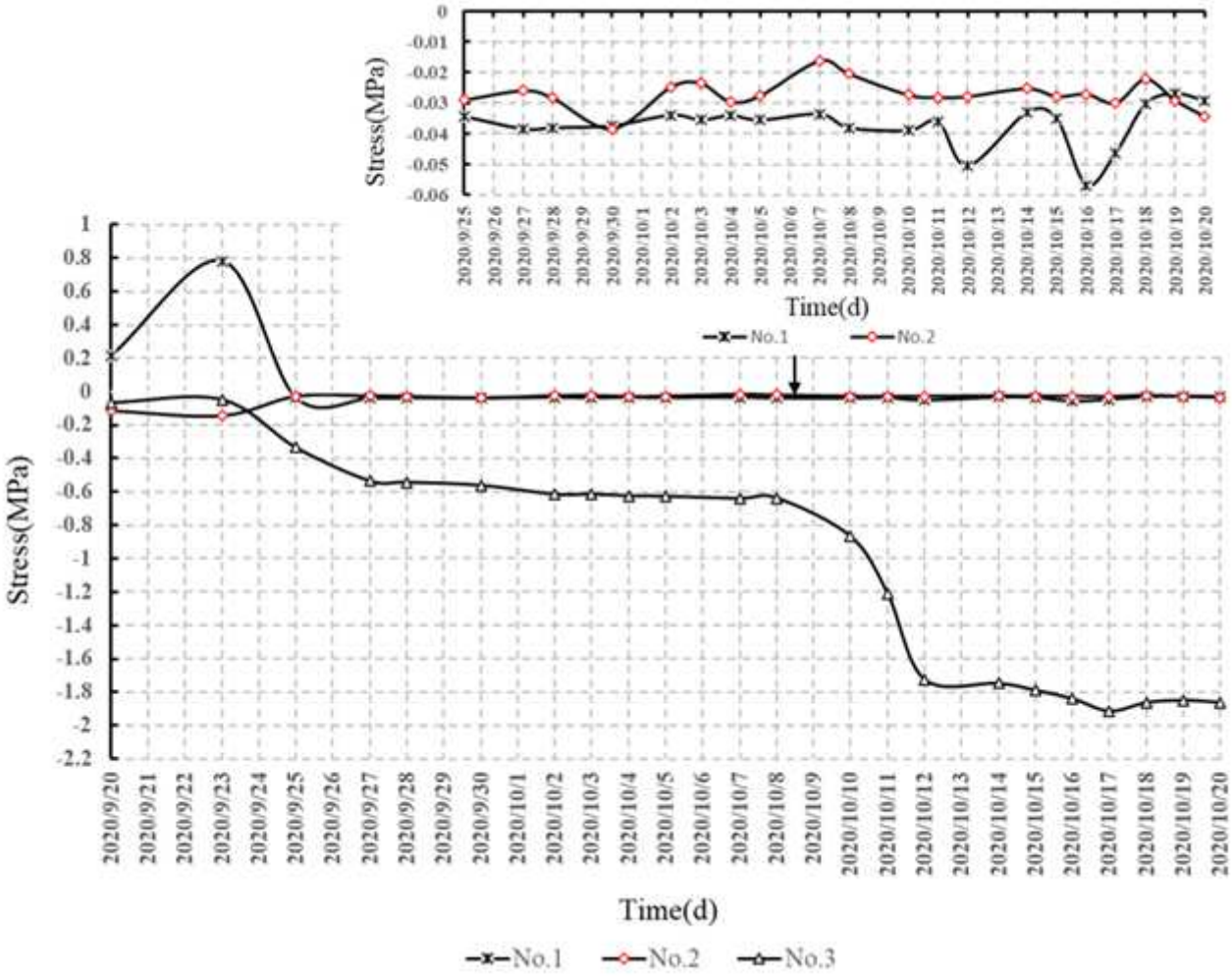

Figure 5

Concrete stress change of -1117.7m shaft lining

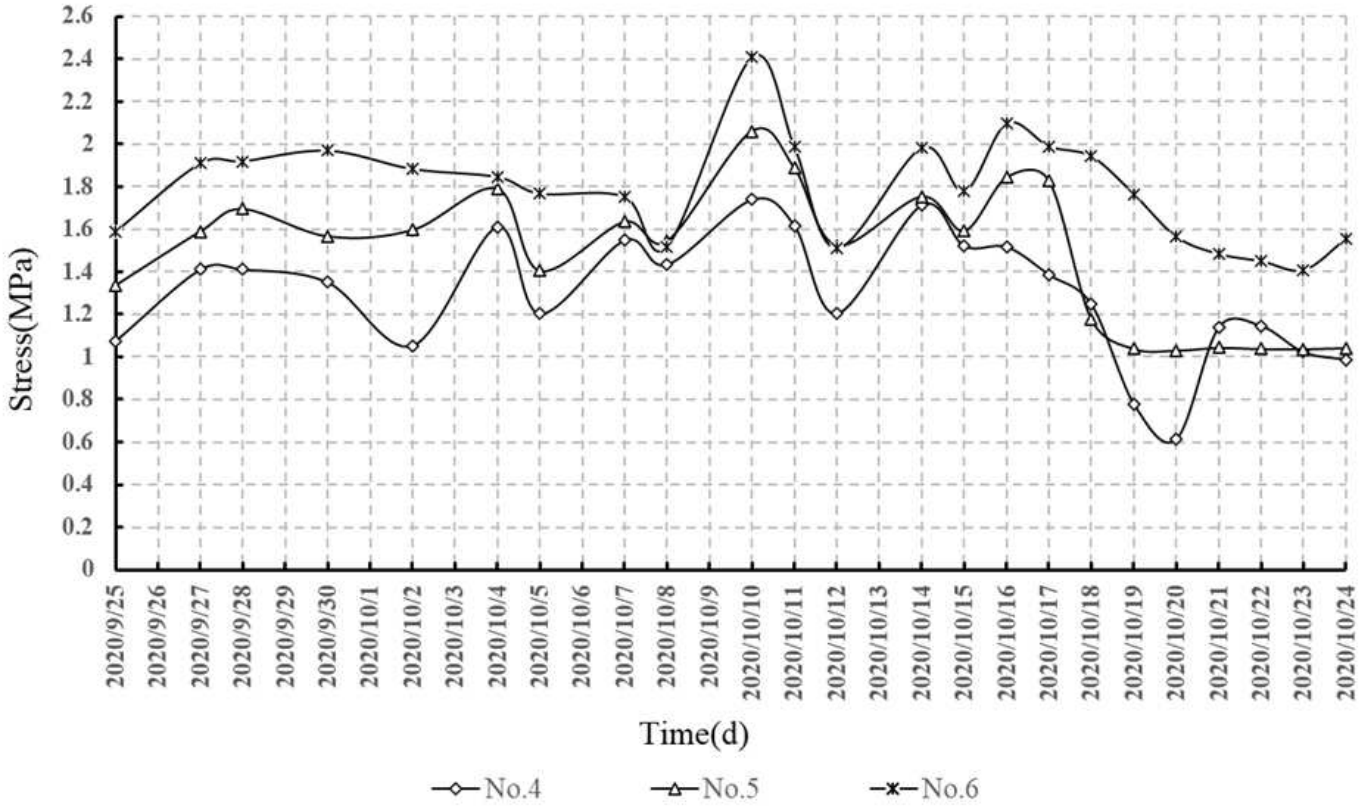

Figure 6

Concrete stress change of -1120m ingate

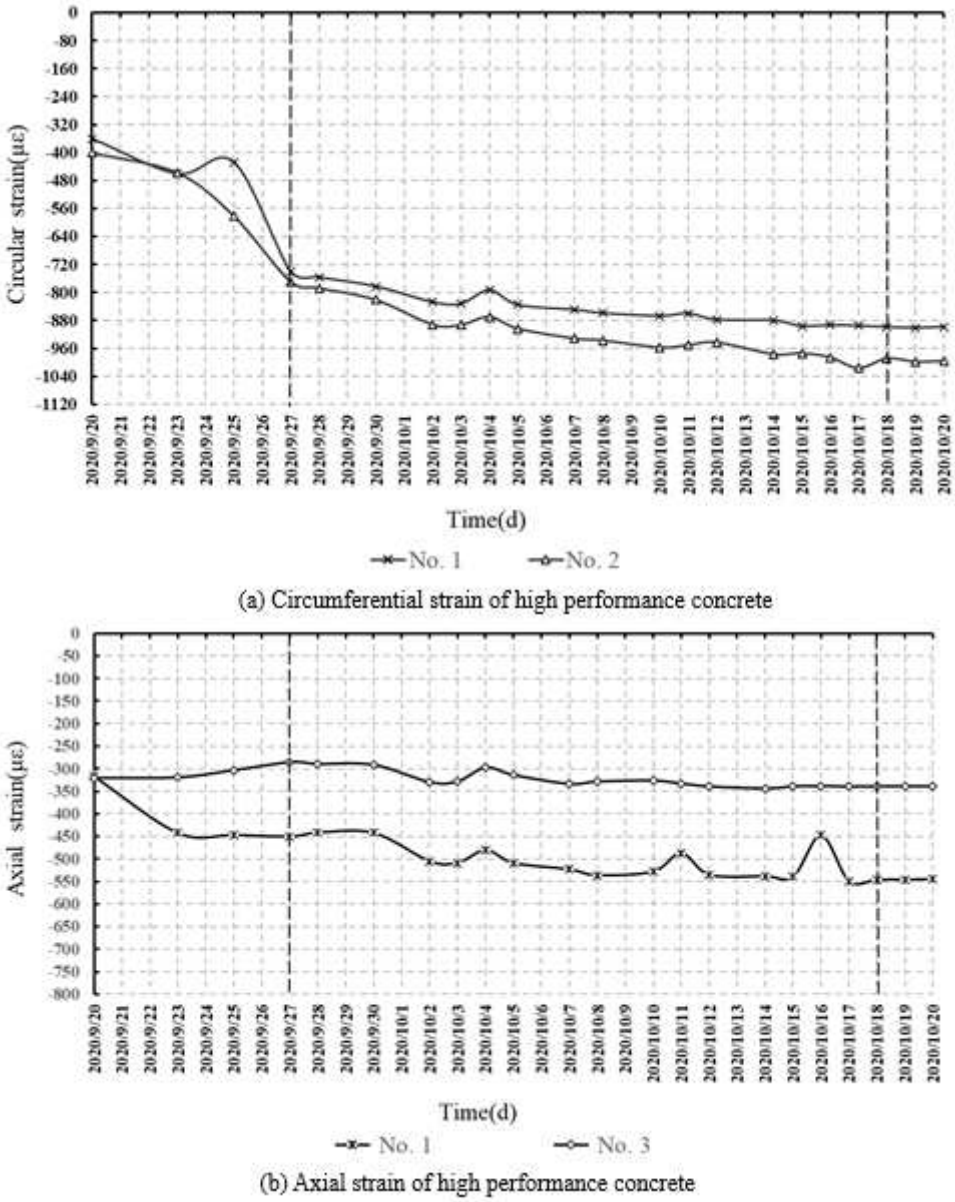

Figure 7

Strain variation of high performance concrete at -1117.7m level

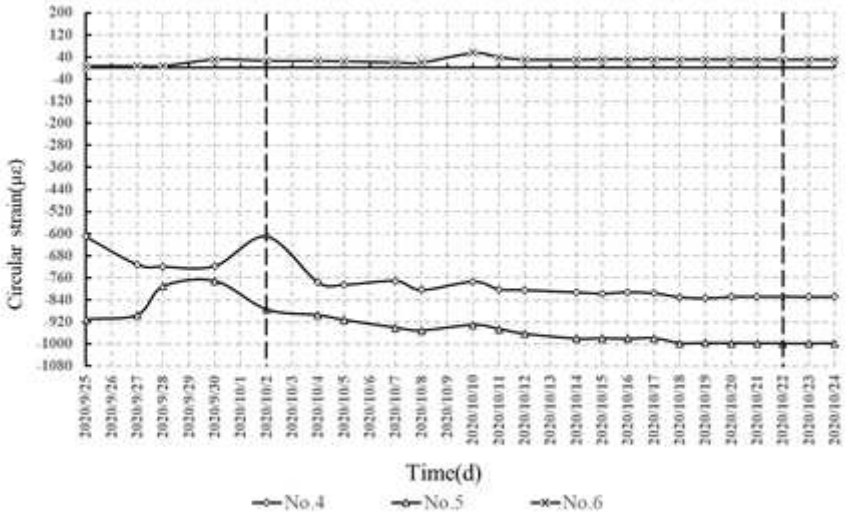

(a) Circumferential strain of high performance concrete for ingate

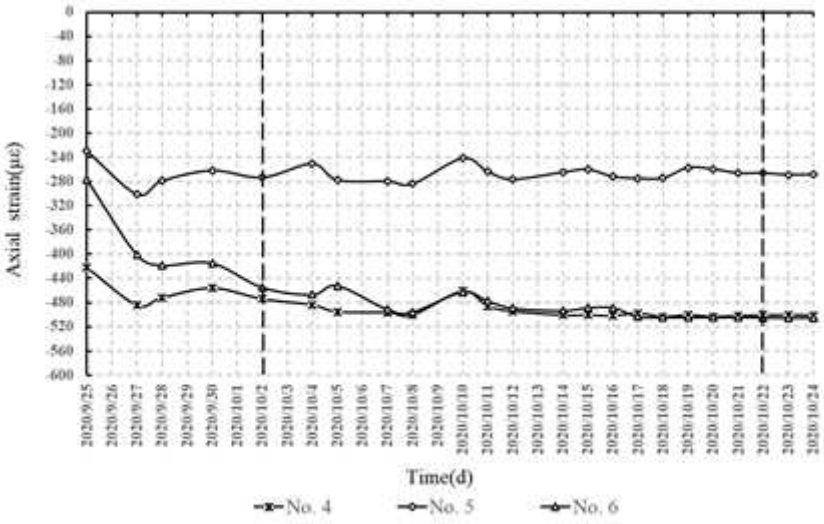

(b) Axial strain of high performance concrete for ingate

Figure 8

Strain variation of high performance concrete for -1120m ingate